Available online at www.sciencedirect.com
ScienceDirect
Biochemical and Biophysical Research Communications 360 (2007) 97–102
BBRC
www.elsevier.com/locate/ybbrc

The crystal structure of FdxA, a 7Fe ferredoxin from *Mycobacterium smegmatis*

Stefano Ricagno [a], Matteo de Rosa [a], Alessandro Aliverti [a], Giuliana Zanetti [a], Martino Bolognesi [a,b,*]

[a] *Department of Biomolecular Sciences and Biotechnology, University of Milano, Via Celoria 26, 20133 Milano, Italy*
[b] *CNR-INFM, c/o Department of Biomolecular Sciences and Biotechnology, University of Milano, Via Celoria 26, 20133 Milano, Italy*

Received 31 May 2007
Available online 12 June 2007

Abstract

Mycobacterium smegmatis ferredoxin FdxA, which has an orthologue ferredoxin in *Mycobacterium tuberculosis*, FdxC, contains both one [3Fe–4S] and one [4Fe–4S] cluster. *M. smegmatis* FdxA has been shown to be a preferred ferredoxin substrate of FprA [F. Fischer, D. Raimondi, A. Aliverti, G. Zanetti, *Mycobacterium tuberculosis* FprA, a novel bacterial NADPH-ferredoxin reductase, Eur. J. Biochem. 269 (2002) 3005–3013], an adrenodoxin reductase-like flavoprotein of *M. tuberculosis*, suggesting that *M. tuberculosis* FdxC could be the physiological partner of the enzyme in providing reducing power to the cytochromes P450. We report here the crystal structure of FdxA at 1.6 Å resolution (R_{factor} 16.5%, R_{free} 20.2%). Besides providing an insight on protein architecture for this 106-residue ferredoxin, our crystallographic investigation highlights lability of the [4Fe–4S] center, which is shown to loose a Fe atom during crystal growth. Due to their high similarity (87% sequence identity), the structure here reported can be considered a valuable model for *M. tuberculosis* FdxC, thus representing a step forward in the study of the complex mycobacterial redox pathways.

Keywords: 7Fe ferredoxin; *Mycobacterium smegmatis*; *Mycobacterium tuberculosis*; Electron transfer; [Fe–S] cluster; [4Fe–4S] cluster instability; Protein structure; X-ray crystallography

Ferredoxins (Fds) are small acidic proteins, containing one or two [Fe–S] clusters. Three kinds of clusters have been described so far in Fds: [2Fe–2S], [3Fe–4S] and [4Fe–4S]. All Fds bearing any of such [Fe–S] clusters act as single-electron carriers in several key metabolic pathways. The 7Fe Fds are present apparently only in bacteria, and display both a cuboidal [3Fe–4S] cluster (cluster I), and a cubane [4Fe–4S] cluster (cluster II) within the same polypeptide chain. The genome of *Mycobacterium tuberculosis* encodes two 7Fe and three 3Fe Fds, respectively [2]. The two 7Fe Fds are thought to be crucial: in particular FdxC was shown to be essential for optimal growth of *M. tuberculosis* [3], whereas FdxA was reported to be induced under conditions of hypoxia and at low pH [4], i.e., under conditions mimicking the environment of the infecting pathogen within macrophages.

In a search for potential protein targets for the design of novel drugs against tuberculosis, FprA, a *M. tuberculosis* adrenodoxin reductase-like enzyme, was functionally and structurally characterized [1,5]. It is worth recalling that in mammals adrenodoxin reductases transfer electrons, by means of a 2Fe Fd, from NADPH to different cytochromes P450 that are involved in key lipid metabolisms; it is also known that *M. tuberculosis* hosts twenty different cytochromes P450 [2]. On these bases, 3Fe and 7Fe Fds from *M. tuberculosis,* that are the presumed physiological substrates of FprA, were therefore overexpressed in *Escherichia coli*, but unfortunately both recombinant Fds failed to yield the functional holoproteins. Thus, we resorted to using FdxA of *M. smegmatis* (MsFd), whose purification had been previously reported [6]. The purified MsFd

* Corresponding author. Fax: +39 02 5031 4895.
E-mail address: martino.bolognesi@unimi.it (M. Bolognesi).

0006-291X/$ - see front matter © 2007 Elsevier Inc. All rights reserved.
doi:10.1016/j.bbrc.2007.06.013

indeed proved to be a very good substrate for FprA, binding the reductase with high affinity [1]. As reported in Fig. 1, the sequence comparison highlights the high similarity linking MsFd and *M. tuberculosis* FdxC, with 87% amino acid identity and several conservative residue substitutions.

To date, four three-dimensional structures of 7Fe Fds have been elucidated. The structure of the *Azotobacter vinelandii* 7Fe Fd (AvFd) was the first described, and currently AvFd is the most thoroughly characterized by means of X-ray crystallographic, electrochemical and spectroscopic methods [19]. More recently, the 7Fe Fds from *Sulfolobus* sp. strain 7, from *Thermus thermophilus* (TtFd) and from *Bacillus schlegelii* (BsFd) have been reported [8–10]. Several 8Fe Fds three-dimensional structures are also available (Table 1). 7Fe and 8Fe Fds can vary in their size from about 55 to 105 amino acids. However, they all share a very similar [Fe–S] cluster-binding core of about 55 amino acids folded according to a conserved $(\beta\alpha\beta)_2$ structure topology. The location of the two [Fe–S] clusters within the binding core is also conserved in 7Fe and 8Fe Fds. Interestingly, the same α–β-fold is found in 4Fe Fds. On the other hand, outside the cluster-binding core, Fds show a higher level of structural variability.

Here we present the 1.6 Å resolution crystal structure of MsFd, the first mycobacterial Fd structure to be reported, and compare its main structural features with known three-dimensional structures of homologous 7Fe Fds. Our data unambiguously show that one Fe atom of the [4Fe–4S] cluster is not present in the crystallized MsFd, suggesting inherent instability of cluster II, which may have undergone a limited oxidative damage during crystal growth.

Materials and methods

Purification of MsFd. Mycobacterium smegmatis cells were grown at 37 °C for 36 h in LB medium supplemented with 0.5% (v/v) glycerol and 0.05% (v/v) Tween 80. MsFd was purified according to the published protocol [6], modified as reported in [1]. Moreover, residual contaminant RNA was removed by a treatment with RNase I. Finally, the protein was stored in 50 mM Tris–HCl, pH 7.4, 0.2 M NaCl. The purified protein showed a single band in SDS–PAGE and a (A_{406}/A_{280}) ratio of 0.6. The protein was quantified using the reported ε_{406} of 26 mM^{-1} cm^{-1} [6].

Crystallisation. MsFd solution was concentrated to a final concentration of 10 mg/ml. In initial crystal screenings, first crystal hits were found after 10 weeks in condition D5 from JBScreen classic 6, Jena bioscience. This crystal hit was further optimized to 3.4 M ammonium sulphate, 1% 2-methyl-2,4-pentanediol, 100 mM sodium acetate, pH 5.5. All crystallisations were performed at 20 °C. While the first screenings were carried out using the Oryx 8 crystallisation robot (Douglas Instruments Ltd., UK) in sitting drop plates, the final optimisation was achieved using the hanging drop technique. MsFd crystallized as dark red rods (about 0.5–1 mm long). Paraffin oil immersion has been adopted as the cryoprotectant procedure. Two diffraction data sets were collected at 110 K, on the same crystal, at the European Synchrotron Radiation Facility (Grenoble) on beam lines ID23A and ID14-3. The first data set was collected at the peak of anomalous scattering for Fe ($\lambda = 1.734$ Å), at 2.15 Å resolution; the second at the remote wavelength $\lambda = 0.931$ Å, at 1.6 Å resolution. Analysis of the diffraction data showed that the MsFd crystals belong to the orthorhombic space group $C222_1$, with unit cell parameters: $a = 54.8$ Å,

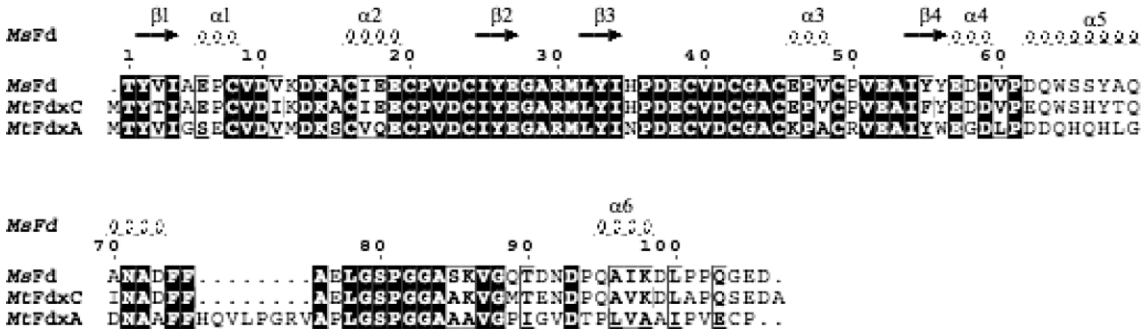

Fig. 1. Sequence alignment of MsFd from *M. smegmatis* with FdxC and FdxA from *M. tuberculosis*. Secondary structure elements of MsFd are reported on top of the alignment.

Table 1
List of all 7Fe and some 8Fe Fds of known three-dimensional structure

[Fe–S] clusters	Organism PDB code	Resolution (Å)	RMSD (AA aligned)	Seq. length	Reference
[4Fe–4S] [3Fe–4S]	*M. smegmatis* this work	1.60 Å	—	106	This work
[4Fe–4S] [3Fe–4S]	*A. vinelandi* 6FD1	1.35 Å	1.9 Å (85)	106	[18]
[4Fe–4S] [3Fe–4S]	*T. thermophilus* 1H98	1.64 Å	0.6 Å (77)	77	[10]
[4Fe–4S] [3Fe–4S]	*B. schlegelii* 1BD6	NMR	1.8 Å (77)	77	[8]
[3Fe–4S] [3Fe–4S] Zn	*Sulfolobus* strain 7 1XER	2.00 Å	1.8 Å (56)	103	[20]
Clostridial 2[4Fe–4S]	*P. asaccharolyticus* 1FDX/1DUR	2.0 Å	0.99 Å (55)	55	[27]
Clostridial 2[4Fe–4S]	*C. pasteurianum* 1CLF	NMR	2.0 Å (55)	55	[28]
Clostridial 2[4Fe–4S]	*C. acidurici* 2FDN	0.94 Å	1.1 Å (55)	55	[29]
Alvin-like 2[4Fe–4S]	*A. vinosum* 1BLU	2.1 Å	1.02 Å (55)	80	[30]
Alvin-like 2[4Fe–4S]	*P. aeruginosa* 2FGO	1.32 Å	2.0 Å (55)	81	[25]

The fourth column lists the RMSD values obtained after superposition of each Fd structure with MsFd (in parentheses the number of matched Cα pairs).

$b = 54.3$ Å, $c = 134.7$ Å, with two molecules in the asymmetric unit. Diffraction data were processed with MOSFLM/SCALA [11,12].

Structure determination and refinement. The MsFd structure was solved by molecular replacement using the Fd of *Thermus thermophilus* (pdb 1H98) [10] as search model and the program MOLREP [13]. Model building and structure inspection were carried out using COOT [14]. The structure was then refined with REFMAC5 [15]. Anomalous maps were calculated with FFT in the CCP4 suite [12]. The MsFd structure was refined at 1.6 Å resolution to a final R-factor value of 16.5% (R-free 20.2%); Table 2 lists the data collection and refinement statistics. Structure alignments were made with SSM [16]. Figures were drawn using Pymol and CCP4MG [17].

Atomic coordinates and structure factors for MsFd have been deposited in Protein Data Bank (pdbcode 2V2K).

Results

Overall structure of MsFd

MsFd is a monomer of 106 amino acids containing one [3Fe–4S] cluster and one [4Fe–4S] cluster. Two independent protein chains (A and B) are present in the crystallographic asymmetric unit, for which 104 and 103 amino acids could be modelled in the electron density, respectively. The electron density is of good quality for both chains and the amino acidic sequence could be unambiguously traced, yielding a high quality model as judged by stereochemical/crystallographic criteria (Table 2). The C-terminal amino acids for which electron density is missing are solvent exposed. Moreover, residual electron density located between residues Cys42 from both chains A and B was observed (Fig. 3a).

MsFd displays the typical $(\beta\alpha\beta)_2$ motif building the [Fe–S] cluster-binding region (residues Thr1–Glu57), consisting of two small, double-stranded, antiparallel β-sheets (β1–β4 and β2–β3) with two α-helices (α2 and α3) packed on one face of the β-sheets (Fig. 2). An additional short α-helix (α1) is present in the middle of loop A. A short α-helix (α4) follows strand β4; the longer α5 helix (residues 65–78) packs onto the opposite face of the β-sheets relative to α2 and α3. The 27 C-terminal amino acids are organized in a loop (loop G), interrupted by helix α6, lying on the surface of the [Fe–S] cluster-binding core (Fig. 2). Both [Fe–S] clusters are located between the two β-sheets and α1, α2, α3 helices. The [3Fe–4S] cluster (cluster I) is coordinated by Cys residues 8, 16, and 49, while cluster II [4Fe–4S] is linked to Cys 20, 39, and 45. Both clusters are inaccessible to the solvent; in particular, cluster I is protected by residues Val11 and Leu32, whereas cluster II is shielded from solvent by the side chain of Tyr2.

Table 2
Data collection and refinement statistics for MsFd

Data collection	Remote dataset	Fe peak
Wavelength (Å)	0.931	1.734
Cell dimensions (Å)	$a = 54.8$ $b = 54.28$ $c = 134.7$	
Resolution (Å)	38-1.60	67–2.15
R_{sym} (%)	7.4 (33.9)	7.3 (32.9)
$I/\sigma I$	12.9 (2.7)	11.5 (5.3)
Completeness (%)	93.9 (99.9)	95.4[a]
Unique reflections	26692 (874)	10621 (1131)
Redundancy	3.5 (3.5)	6.1[a]
Refinement		
R_{work} (%)	16.5	
R_{free} (%)	20.2	
Number of atoms		
Protein	1640	
Solvent	118	
Ramachandran plot (%)		
Most favoured region	88.3	
Additional allowed region	11.7	
Generously allowed region	0.0	
Disallowed region	0.0	

Statistics in parentheses refer to the high resolution shell (1.60–1.69 Å for the remote dataset; 2.15–2.27 Å for the anomalous peak dataset).

[a] Anomalous completeness and redundancy are given.

Inspection of the MsFd refined electron density shows unexpectedly that in the crystallized structure one Fe atom is not present in cluster II. Furthermore, the side chain of Cys42, which normally coordinates the fourth Fe atom in the 7Fe and 8Fe Fds, is pointing away from cluster II, towards the solvent and the neighbouring protein molecule in the crystal asymmetric unit. Such conformation adopted by Cys42 (in both A and B chains) matches part of the unexplained residual electron density observed during the refinement. Structural and sequence searches (DALI and BLAST) against the Protein Data Bank showed that AvFd, TtFd and BsFd three-dimensional structures are those that match most closely that of MsFd. All three Fds contain a [4Fe–4S] cluster whose Cys residues are conserved and essentially structured as in MsFd [8,10,18], while keeping all the four Fe atoms of cluster II.

7Fe Fds are known to be thermo- and air-stable [Fe–S] protein [19]. Nevertheless, some evidence of the conversion of the 7Fe Fd [4Fe–4S] cluster into a [3Fe–4S] cluster under particular conditions has been reported. The crystal structure of the 7Fe Fd from *Sulfolbus* sp strain 7 [20] clearly shows that the [4Fe–4S] cluster II is present in this protein as a [3Fe–4S] cluster. Furthermore, while isolating MsFd, Imai et al. [21] purified a second Fd species containing only six Fe atoms. Such 6Fe Fd species turned out to be a modified form of MsFd, which had undergone partial oxidative degradation during the rather long purification procedure [9,21]. More recently, the recombinant 7Fe Fds of *Bacillus thermoproteolyticus* have been characterized, showing once more a conversion of cluster II to a [3Fe–4S] form. The crystal structure of one of these 6Fe modified Fds shows that the Cys residue, corresponding to Cys42 in MsFd, bears a covalently bound molecule of coenzyme A through a disulfide bond [22]. Thus, under particular conditions, oxygen can destabilize the [4Fe–4S] cluster, resulting in the loss of one Fe atom and in a conformational change that regularly affects the second Cys residue of the cluster-binding motif Cys-X_2-Cys-X_2-Cys. Such reactive Cys residue (Cys42 in MsFd) reorients its side-chain towards the solvent and may form disulfide bonds or be further oxidized. Interestingly, such selective

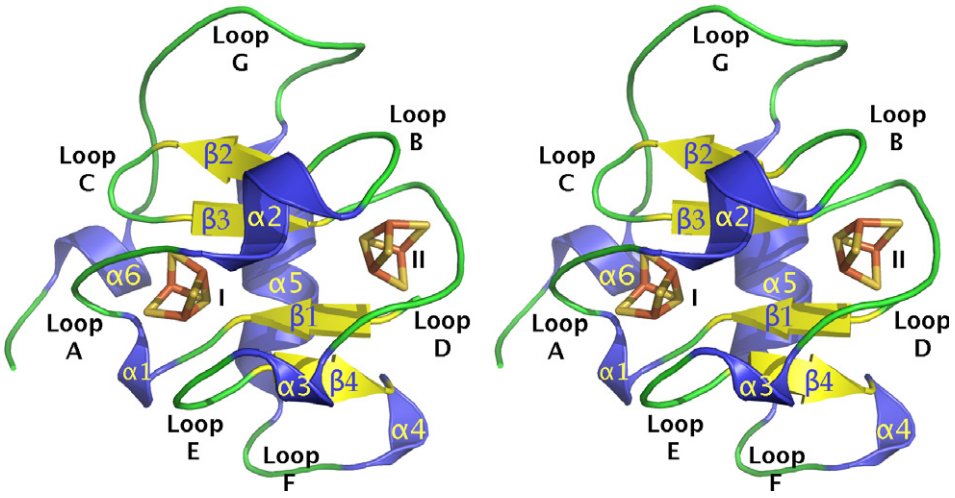

Fig. 2. Cartoon representation of MsFd from *M. smegmatis* in stereo view. The two [Fe–S] clusters are identified as I and II. All secondary structure elements and loops are labelled; α-helical regions are shown in blue, the β-strands in yellow. (For interpretation of the references to colour in this figure legend, the reader is referred to the web version of this article.)

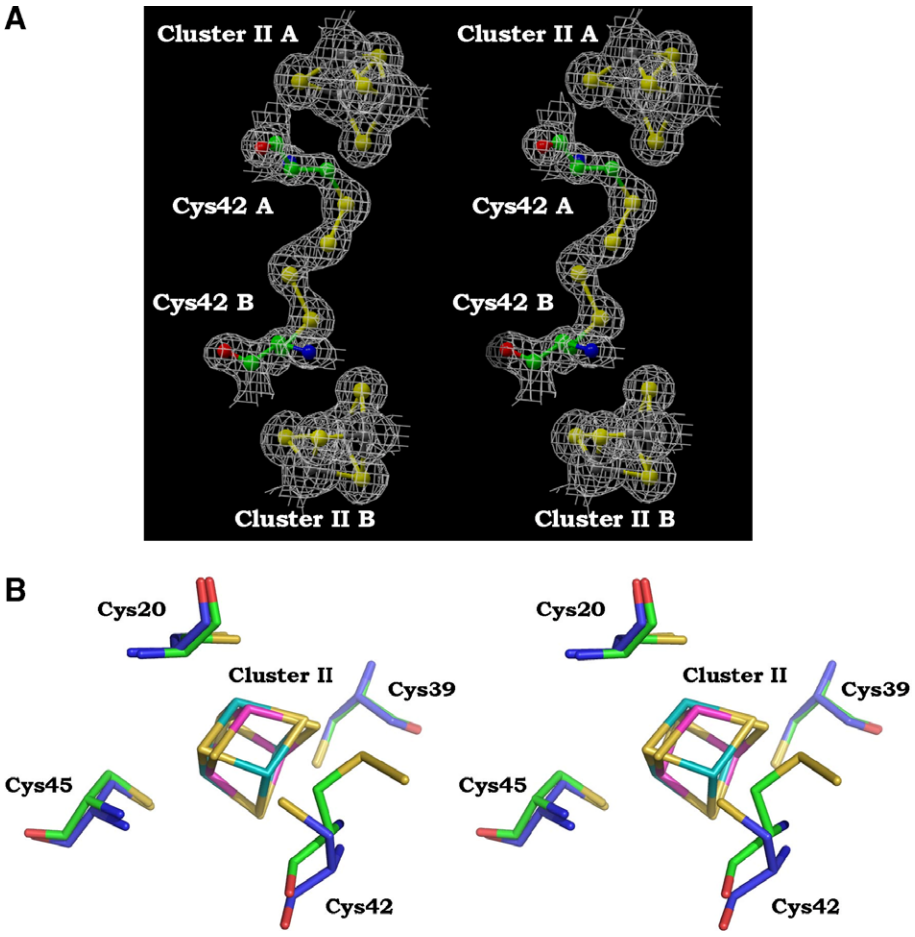

Fig. 3. (A) Ball and stick representation of Cys42 and cluster II from molecules A and B. The electron density for the refined model (contoured at 1.5σ) is shown. (B) Superposition of cluster II in MsFd (magenta) and TtFd (cyan). Cys residues coordinating cluster II from MsFd and TtFd are shown in green and blue, respectively; MsFd Cys42 has flipped away from cluster II, and the corresponding Fe atom is absent. (For interpretation of the references to colour in this figure legend, the reader is referred to the web version of this article.)

conversion of cluster II does not destabilize cluster I, nor has sizeable effects on the overall protein structure [9,22]. It must additionally be recalled that in 7Fe Fds the redox functional role has been assigned to the [3Fe–4S] cluster I, whereas cluster II is believed to play only a structural function [23,19].

The packing of two MsFd molecules in the crystal asymmetric unit brings Cys42 of chains A and B in close spatial proximity (Cα–Cα distance of 7.3 Å). As mentioned above, the refined crystal structure shows significant residual electron density located between these two residues, roughly comparable to the density that one would expect for an intermolecular covalent cross-bridge (Fig. 3). The distance between the SD atoms of Cys42 of chains A and B is however 5.20 Å, thus ruling out the possibility of a direct covalent bond between the two SD atoms contributed by the two protein chains. To shed light on the chemical nature of such intermolecular cross-bridge we first calculated an anomalous difference map based on the Fe anomalous contribution; such electron density map promptly located 6Fe atoms, but did not show any peak outside the two [Fe–S] clusters, ruling out the presence of Fe atoms in the Cys42 cross-bridge. The extra density at residue 42 was then modelled as hydroxyl-Cys, or persulfide-Cys. In the first case residual electron density was present after refinement on the modelled oxygen atoms and between the two Cys residues; furthermore, the distance between the putative O atom and SD was 2.0 Å, i.e., too long for a S–O bond. When Cys42 was modelled as persulfide-Cys, it showed a good stereochemistry for the SD–SE bond (SE is the persulfide S atom), with a SD–SE bond length of 2.05 Å, the distance between the putative SE atoms provided by chains A and B being however 3.0 Å. Although some residual density was still visible between the two putative SE atoms, additional atoms could not be modelled. The above observations therefore suggest that the extra electron density observed between the Cys42 residues from the A and B chains may represent differently modified/oriented Cys species (including persulfide Cys), that may originate from a combination of air oxidation during crystal growth and X-ray radiation damage (at $\lambda = 1.734$ Å).

Comparison with other ferredoxins

All 7Fe and 8Fe Fds are phylogenetically related [24]. They display a high degree of structural homology showing the same common cluster-binding core of about 55 amino acids, based on the $(\beta\alpha\beta)_2$ motif. The conservation of the cluster-binding core is evident at the primary and tertiary structure levels in all 7Fe and 8Fe Fds (Table 1). The shortest Fds consist essentially of the cluster-binding core, whereas Fds composed of about 75–80 amino acids display a C-terminal α-helix corresponding to α5 of MsFd; such a helix is a characteristic structural feature of 7Fe thermostable Fds [10], being easily superimposable in all 7Fe Fds. MsFd three-dimensional structure can be superimposed on 8Fe Fd structures only for the minimal 55-residue core (Table 1 and Fig. 4). For example, although the 8Fe Fd from *Pseudomonas aeruginosa* presents a C-terminal helix, this does not match the location of MsFd α5 helix (Fig. 4) [25]. 7Fe Fds from mesophilic bacteria are often characterized by 30 C-terminal amino acids following the α5 helix [10]; to date the structure of 7Fe AvFd has been the only one available within such class [18]. MsFd and AvFd superimpose well for 85 residues, including the α5 helix. However, their C-terminal residues, consisting of a long loop and an α-helix, are not superimposable and contact different sites of the Fd core (Table 1 and Fig. 4). While the cluster-binding core is sufficient for the effective binding of two [Fe–S] clusters, the function of the C-terminal extension remains elusive, despite the extensive characterization of AvFd [26]. In light of its sequence and structural variability, it can be speculated that the C-terminal region may be crucial for the interaction of MsFd with either its reductase or its electron acceptor(s). Experimental evidence in this direction is however lacking. It seems less likely that the C-termini of MsFd and AvFd might play any role in tuning the protein redox potentials, since they are not involved in interactions with the [Fe–S] clusters.

As mentioned above, MsFd displays 87% amino acid sequence identity with *M. tuberculosis* FdxC (Fig. 1). Since the similarity between the two Fds is high, MsFd crystal structure may be regarded as a reliable model for *M. tuberculosis* FdxC. In our previous studies, MsFd has been identified, among various Fds, as the best electron-acceptor substrate of *M. tuberculosis* FprA [1]. Thus, it has been

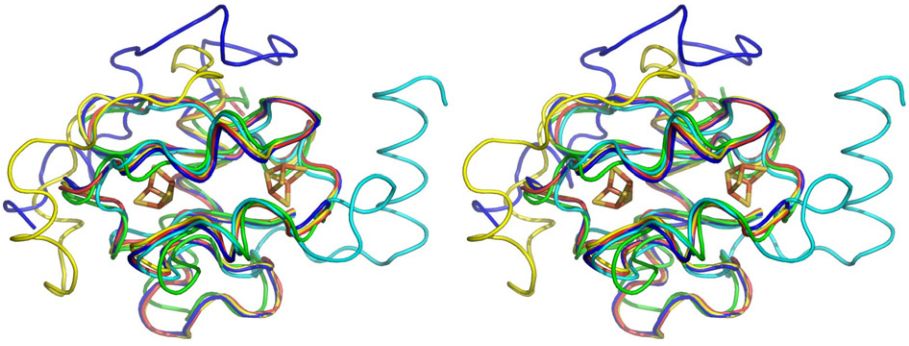

Fig. 4. (a) Superposition of MsFd (blue) with other 7Fe Fds: AvFd (yellow), BsFd (green), TtFd (red), and the 8Fe Fd from *Pseudomonas aeruginosa* (PaFd) (cyan). Only the MsFd [Fe–S] clusters are shown. BsFd and TtFd structures match nicely, while PaFd displays a C-terminal helix differently oriented relative to the α5 helix. MsFd (blue) and AvFd (yellow) are well superimposed between amino acids 1–85, while the C-terminal 30 amino acids are entirely differently structured. Protein structures are oriented similarly as in Fig. 2. (For interpretation of the references to colour in this figure legend, the reader is referred to the web version of this article.)

suggested that the *M. tuberculosis* FprA/FdxC system could provide reducing equivalents to (at least) some of the many cytochromes P450 in the pathogen. In this respect, the structure of MsFd is one further step in the direction of gaining insight on *M. tuberculosis* metabolic-redox pathways.

Acknowledgments

This work was supported by grants from Fondazione Cariplo, Milano, Italy and MIUR (Prin 2005). S.R. is a youg-research-fellow of the MIUR Project "Biologia Strutturale" (FIRB 2003). M.B. is grateful to CIMAINA (Excellence Center, University of Milano) for continuous support. Dr. Gerlind Sulzenbacher (AFMB, CNRS, Marseille) and Raffaele Cerutti are gratefully acknowledged for technical help. European Synchrotron Radiation Facility (Grenoble) is also acknowledged for synchrotron time.

References

[1] F. Fischer, D. Raimondi, A. Aliverti, G. Zanetti, *Mycobacterium tuberculosis* FprA, a novel bacterial NADPH-ferredoxin reductase, Eur. J. Biochem. 269 (2002) 3005–3013.
[2] http://genolist.pasteur.fr/TubercuList/.
[3] C.M. Sassetti, D.H. Boyd, E.J. Rubin, Genes required for mycobacterial growth defined by high density mutagenesis, Mol. Microbiol. 48 (2003) 77–84.
[4] D.R. Sherman, M. Voskuil, D. Schnappinger, R. Liao, M.I. Harrell, G.K. Schoolnik, Regulation of the *Mycobacterium tuberculosis* hypoxic response gene encoding alpha-crystallin, Proc. Natl. Acad. Sci. USA 98 (2001) 7534–7539.
[5] R.T. Bossi, A. Aliverti, D. Raimondi, F. Fischer, G. Zanetti, D. Ferrari, N. Tahallah, C.S. Maier, A.J. Heck, M. Rizzi, A. Mattevi, A covalent modification of NADP+ revealed by the atomic resolution structure of FprA, a *Mycobacterium tuberculosis* oxidoreductase, Biochemistry 41 (2002) 8807–8818.
[6] T. Imai, T. Matsumoto, S. Ohta, D. Ohmori, K. Suzuki, J. Tanaka, M. Tsukioka, J. Tobari, Isolation and characterization of a ferredoxin from *Mycobacterium smegmatis* Takeo, Biochim. Biophys. Acta 743 (1983) 91–97.
[8] S. Aono, D. Bentrop, I. Bertini, A. Donaire, C. Luchinat, Y. Niikura, A. Rosato, Solution structure of the oxidized Fe7S8 ferredoxin from the thermophilic bacterium *Bacillus schlegelii* by 1H NMR spectroscopy, Biochemistry 37 (1998) 9812–9826.
[9] T. Iwasaki, E. Watanabe, D. Ohmori, T. Imai, A. Urushiyama, M. Akiyama, Y. Hayashi-Iwasaki, N.J. Cosper, R.A. Scott, Spectroscopic investigation of selective cluster conversion of archaeal zinc-containing ferredoxin from *Sulfolobus* sp. strain 7, J. Biol. Chem. 275 (2000) 25391–25401.
[10] S. Macedo-Ribeiro, B.M. Martins, P.J. Pereira, G. Buse, R. Huber, T. Soulimane, New insights into the thermostability of bacterial ferredoxins: high-resolution crystal structure of the seven-iron ferredoxin from *Thermus thermophilus*, J. Biol. Inorg. Chem. 6 (2001) 663–674.
[11] A.G.W. Leslie, Recent changes to the MOSFLM package for processing film and image plate data, Joint CCP4 + ESF-EAMCB Newsletter on Protein Crystallography (1992).
[12] CCP4, The CCP4 suite: programs for protein crystallography, Acta Crystallogr. D. Biol. Crystallogr. 50 (1994) 760–763.
[13] A.A. Vagin, A. Teplyakov, MOLREP: an automated program for molecular replacement, J. Appl. Crystallogr. (1997) 1022–1025.
[14] P. Emsley, K. Cowtan, Coot: model-building tools for molecular graphics, Acta Crystallogr. D. Biol. Crystallogr. 60 (2004) 2126–2132.
[15] G.N. Murshudov, A.A. Vagin, E.J. Dodson, Refinement of macromolecular structures by the maximum-likelihood method, Acta Crystallogr. D. Biol. Crystallogr. 53 (1997) 240–255.
[16] E. Krissinel, K. Henrick, Secondary-structure matching (SSM), a new tool for fast protein structure alignment in three dimensions, Acta Crystallogr. D. Biol. Crystallogr. 60 (2004) 2256–2268.
[17] L. Potterton, S. McNicholas, E. Krissinel, J. Gruber, K. Cowtan, P. Emsley, G.N. Murshudov, S. Cohen, A. Perrakis, M. Noble, Developments in the CCP4 molecular-graphics project, Acta Crystallogr. D. Biol. Crystallogr. 60 (2004) 2288–2294.
[18] C.D. Stout, E.A. Stura, D.E. McRee, Structure of *Azotobacter vinelandii* 7Fe ferredoxin at 1.35 A resolution and determination of the [Fe–S] bonds with 0.01 A accuracy, J. Mol. Biol. 278 (1998) 629–639.
[19] C.D. Stout, Ferredoxins containing two different Fe/S centers of the forms [4Fe–4S] and [3Fe–4S], in: A. Messerschmidt, R. Huber, T. Poulos, K. Wieghardt (Eds.), Handbook of Metalloproteins, Wiley & Sons Ltd., Chichester, 2001, pp. 560–574.
[20] T. Fujii, Y. Hata, T. Wakagi, N. Tanaka, T. Oshima, Novel zinc-binding centre in thermoacidophilic archaeal ferredoxins, Nat. Struct. Biol. 3 (1996) 834–837.
[21] T. Imai, A. Urushiyama, H. Saito, Y. Sakamoto, K. Ota, D. Ohmori, A novel 6Fe ($2 \times$ [3Fe-4S]) ferredoxin from *Mycobacterium smegmatis*, FEBS Lett. 368 (1995) 23–26.
[22] T. Shirakawa, Y. Takahashi, K. Wada, J. Hirota, T. Takao, D. Ohmori, K. Fukuyama, Identification of variant molecules of *Bacillus thermoproteolyticus* ferredoxin: crystal structure reveals bound coenzyme A and an unexpected [3Fe–4S] cluster associated with a canonical [4Fe–4S] ligand motif, Biochemistry 44 (2005) 12402–12410.
[23] T. Iwasaki, T. Wakagi, Y. Isogai, K. Tanaka, T. Iizuka, T. Oshima, Functional and evolutionary implications of a [3Fe–4S] cluster of the dicluster-type ferredoxin from the thermoacidophilic archaeon, Sulfolobus sp. strain 7, J. Biol. Chem. 269 (1994) 29444–29450.
[24] K. Fukuyama, H. Matsubara, T. Tsukihara, Y. Katsube, Structure of [4Fe–4S] ferredoxin from *Bacillus thermoproteolyticus* refined at 2.3 A resolution. Structural comparisons of bacterial ferredoxins, J. Mol. Biol. 210 (1989) 383–398.
[25] P. Giastas, N. Pinotsis, G. Efthymiou, M. Wilmanns, P. Kyritsis, J.M. Moulis, I.M. Mavridis, The structure of the 2[4Fe–4S] ferredoxin from *Pseudomonas aeruginosa* at 1.32-A resolution: comparison with other high-resolution structures of ferredoxins and contributing structural features to reduction potential values, J. Biol. Inorg. Chem. 11 (2006) 445–458.
[26] Y.S. Jung, V.A. Roberts, C.D. Stout, B.K. Burgess, Complex formation between *Azotobacter vinelandii* ferredoxin I and its physiological electron donor NADPH-ferredoxin reductase, J. Biol. Chem. 274 (1999) 2978–2987.
[27] E.T. Adman, L.C. Siefker, L.H. Jensen, Structure of *Peptococcus aerogenes* ferredoxin. Refinement at 2 A resolution, J. Biol. Chem. 251 (1976) 3801–3806.
[28] I. Bertini, A. Donaire, B.A. Feinberg, C. Luchinat, M. Piccioli, H. Yuan, Solution structure of the oxidized 2[4Fe–4S] ferredoxin from *Clostridium pasteurianum*, Eur. J. Biochem. 232 (1995) 192–205.
[29] Z. Dauter, K.S. Wilson, L.C. Sieker, J. Meyer, J.M. Moulis, Atomic resolution (0.94 A) structure of *Clostridium acidurici* ferredoxin. Detailed geometry of [4Fe–4S] clusters in a protein, Biochemistry 36 (1997) 16065–16073.
[30] J.M. Moulis, L.C. Sieker, K.S. Wilson, Z. Dauter, Crystal structure of the 2[4Fe-4S] ferredoxin from *Chromatium vinosum*: evolutionary and mechanistic inferences for [3/4Fe–4S] ferredoxins, Protein Sci. 5 (1996) 1765–1775.